Acta Crystallographica Section C
Crystal Structure Communications
ISSN 0108-2701

Sorafenib and its tosylate salt: a multikinase inhibitor for treating cancer

K. Ravikumar,[a]* B. Sridhar,[a] A. K. S. Bhujanga Rao[b] and M. Pulla Reddy[b]

[a]Laboratory of X-ray Crystallography, Indian Institute of Chemical Technology, Hyderabad 500 007, India, and [b]Natco Research Centre, Sanath Nagar, Hyderabad 500 018, India
Correspondence e-mail: sshiya@yahoo.com

Received 10 November 2010
Accepted 16 November 2010
Online 8 December 2010

Sorafenib, a drug that targets malignant cancer cells and cuts off the blood supply feeding the tumour, has been crystallized as the free base, 4-(4-{3-[4-chloro-3-(trifluoromethyl)phenyl]-ureido}phenoxy)-*N*-methylpyridine-2-carboxamide, $C_{21}H_{16}ClF_3N_4O_3$, (I), and as a tosylate salt, 4-(4-{3-[4-chloro-3-(trifluoromethyl)phenyl]ureido}phenoxy)-2-(*N*-methylcarbamoyl)pyridinium 4-methylbenzenesulfonate, $C_{21}H_{17}ClF_3N_4O_3^+\cdot C_7H_7O_3S^-$, (II). In both structures, the sorafenib molecule is in an extended conformation. The pyridine-2-carboxamide group exhibits a *syn* conformation of the N atoms in (I), whereas an almost *anti* orientation is present in (II). In both crystal structures, the two terminal groups, *viz.* pyridine-2-carboxamide and the trifluorophenyl ring, are oriented differently to the conformations found in enzyme-bound sorafenib. The sorafenib molecules in (I) are linked into zigzag chains by N—H···O hydrogen bonds, whereas in (II) the presence of the additional tosylate anion results in the formation of chains of fused hydrogen-bonded rings. This study reveals the variations in the solid-state conformation of the sorafenib molecule in different crystalline environments.

Comment

Angiogenesis, the formation of new blood vessels from existing vasculature, is required for tumour growth and metastasis, and the concept of inhibiting tumour angiogenesis has become a compelling approach in the development of anticancer agents (Ferrara & Kerbal, 2005). Vascular endothelial growth factor (VEGF) is a known promoter of angiogenesis, and the increased expression of VEGF has been implicated in tumour growth and metastasis (Yancopoulos *et al.*, 2000). VEGF signalling through its three tyrosine kinase receptors (RTK), *viz.* VEGFR-1, VEGFR-2 and VEGFR-3, promotes several events required for the formation of new blood vessels, such as endothelial cell survival, proliferation and migration, and vascular permeability (Holmes *et al.*, 2007). Therefore, the blockage of VEGF signalling by small-molecule inhibitors, particularly at the VEGFR-2 kinase domain, has been shown to be an attractive strategy in the treatment of cancers (Ferrara *et al.*, 2004).

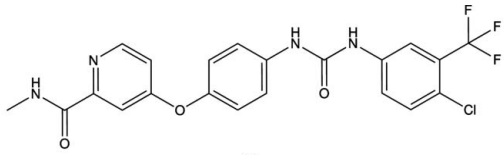

(I)

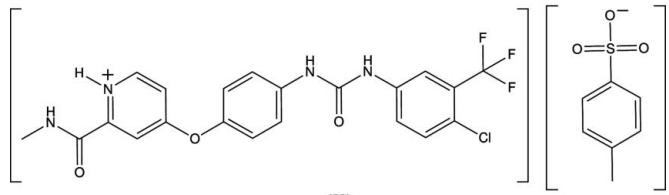

(II)

Sorafenib is an oral multikinase inhibitor acting on tumour cells and cells of the tumour vasculature. It also inhibits tumour cell proliferation by targeting the mitogen-activated protein kinase pathway at the level of RAF kinase (Wilhelm *et al.*, 2004). Sorafenib is approved for use in advanced renal cell carcinoma (primary kidney cancer) when anticancer treatment with interferon-α or interleukin-2 has failed or cannot be used (Escudier *et al.*, 2007). In 2007, the US Food and Drug Administration (FDA) approved sorafenib tosylate (BAY43–9006, Nexavar, 200 mg tablets; Bayer Pharmaceuticals Corporation, Montville, New Jersey, USA, and Onyx Pharma-

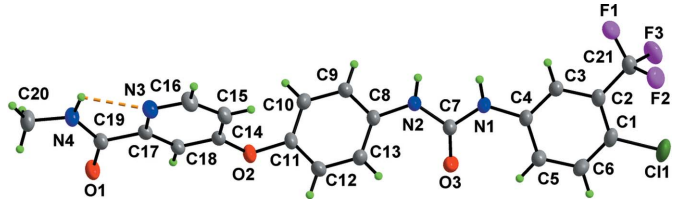

Figure 1
The asymmetric unit of (I), showing the atom-numbering scheme. Displacement ellipsoids are drawn at the 30% probability level and H atoms are shown as small spheres of arbitrary radii. The dashed line indicates the intramolecular hydrogen bond.

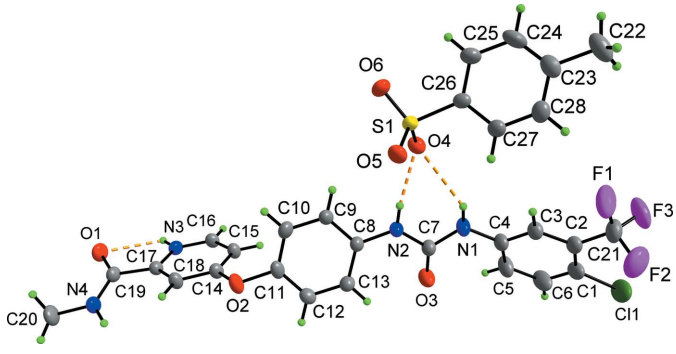

Figure 2
The asymmetric unit of (II), showing the atom-numbering scheme. Displacement ellipsoids are drawn at the 30% probability level and H atoms are shown as small spheres of arbitrary radii. Hydrogen bonds are shown as dashed lines.

 doi:10.1107/S0108270110047451

ceuticals Corporation, Emeryville, California, USA), an oral kinase inhibitor, for the treatment of patients with unresectable hepatocellular carcinoma (Kane *et al.*, 2009). As part of our ongoing structural studies of pharmaceutical compounds (Ravikumar *et al.*, 2008; Ravikumar & Sridhar, 2009, 2010), the crystal structures of sorafenib, (I), and its tosylate salt, (II), have been determined and are reported here.

The sorafenib molecule consists of a derivative of a biarylurea joined to a pyridine-2-carboxamide group. Both compounds (I) and (II) crystallize in the space group $P2_1/c$. Views of the asymmetric units of (I) and (II), with atom labelling, are presented in Figs. 1 and 2, respectively. The urea linkage plays an active role in the solid-state conformation and governs the overall shape of the sorafenib molecule, which is in an extended conformation in both structures. Atom N3 of the pyridine ring is protonated to form the pyridinium cation in (II); the sum of the angles at this atom is 356.4 (1)°. There are significant variations in the bond lengths and angles displayed by the pyridine-2-carboxamide group of (I) compared with those of (II) as a consequence of the protonation in the latter (Table 1). The intra-ring angle at atom N3 is about 6° larger in (II) than in (I), while the intra-ring angles at atoms C16 and C17 decrease by about 4 and 5°, respectively. The pyridine ring bonds, except C15—C14, and the bonds involving atom C19 are significantly shorter in (II) than in the free base, (I). Other differences in the bond angles at atoms C17 and C19 (Table 1) suggest there may be some repulsion between atoms H4N and H18 in (II), while this interaction is not present in (I), as well as a stronger interaction involving N3—H···O1 in (II) compared with N4—H···N3 in (I).

The pyridine-2-carboxamide group exhibits a *syn* conformation of the N atoms in (I), while an almost *anti* orientation is present in (II). These orientations are likely to be favoured because they facilitate the formation of an intramolecular hydrogen bond, *viz.* N4—H···N3 in (I) and N3—H···O1 in (II), whereas the reverse conformation in each structure would obviate any intramolecular hydrogen bonds.

Fig. 3 shows an overlay of the sorafenib molecules of (I) and (II) with sorafenib ligands extracted from the crystal structures of complexes of sorafenib bound to the human P38 MAP kinase [Simard *et al.* (2009), Protein Data Bank (PDB; Berman *et al.*, 2000) entry 3GCS; Namboodiri *et al.* (2010),

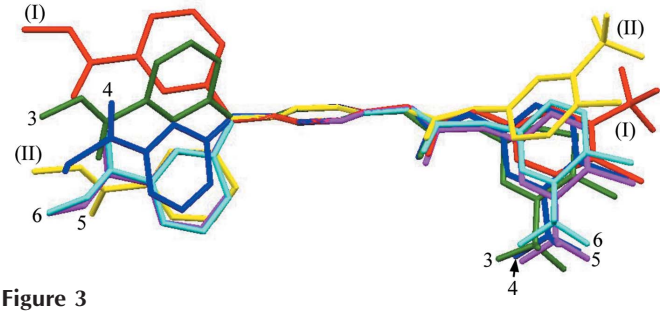

Figure 3
A superposition of the molecular conformations of the sorafenib molecules. The overlay was produced by making a least-squares fit of the central planar six-membered ring atoms with those of (I). The labels are as follows: (II) is sorafenib tosylate; 3 is PDB code 3GCS; 4 is 3HEG; 5 is 1UWH (molecule 1); 6 is 1UWH (molecule 2).

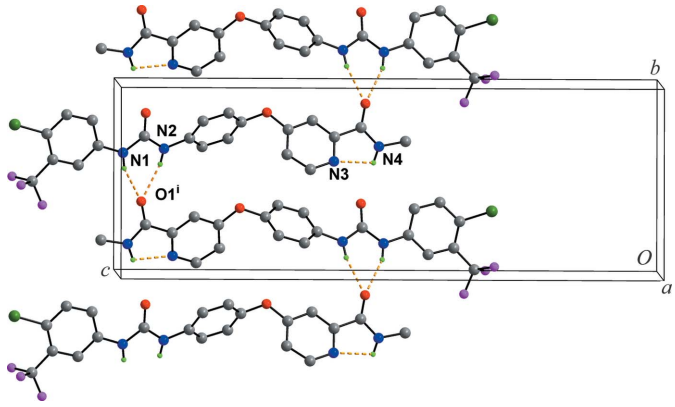

Figure 4
Part of the crystal packing of (I), showing the zigzag hydrogen-bonded chain. Hydrogen bonds are shown as dashed lines and H atoms not involved in hydrogen bonding have been omitted for clarity. Selected atoms of the molecules present in the asymmetric unit are labelled, primarily to provide a key for the coding of the atoms. [Symmetry code: (i) $-x+1, y-\frac{1}{2}, -z+\frac{3}{2}$.]

PDB entry 3HEG] and B-RAF kinase [Wan *et al.* (2004), PDB entry 1UWH]. The conformational flexibility provided by the urea and ether linkages in the sorafenib molecule allows the terminal groups in the free and enzyme-bound molecules to adopt different orientations (Table 2). It is interesting to note that, in the enzyme-bound sorafenib molecules, the binding mode requires the pyridine-2-carboxamide group to adopt a *syn* orientation. It can be seen that the lipophilic trifluorophenyl ring in the enzyme-bound sorafenib molecules always has roughly the same conformation, whereas quite different orientations are found in (I) and (II). As observed by Wan *et al.* (2004), the conformation in the enyme-bound molecule may be necessary to provide favourable hydrophobic interactions at the active site. On the other hand, the conformation of the pyridine-2-carboxamide group seems to be quite variable, which suggests that different hydrogen-bonding interactions in the bound and unbound forms may influence the conformation of the hydrophilic end of the molecule.

The least-squares plane of the trifluorophenyl ring is more inclined to the pyridyl plane in (II) [69.5 (1)°] than in (I) [40.1 (1)°], perhaps to accommodate the tosylate anion by allowing both urea N atoms to be involved in hydrogen bonds with the anion. The phenyl ring in the tosylate anion makes almost equal dihedral angles of 51.7 (1) and 59.0 (1)° with the planes of the trifluorophenyl and pyridyl rings, respectively.

The crystal packing in (I) and (II) is influenced by the N—H···O hydrogen bonds (Tables 3 and 4). Both atoms N1 and N2 of the urea group in (I) form hydrogen bonds with atom O1 of the carboxamide group of a neighbouring molecule, forming zigzag chains of molecules which run along the *b* axis (Fig. 4). It is interesting to see that, in (II), each tosylate anion, as acceptor, links three sorafenib molecules by participating in all the N—H···O hydrogen bonds (Fig. 5). Combination with the interaction involving protonated atom N3 [N3—H···O5($-x+2, y+\frac{1}{2}, -z+\frac{3}{2}$)] of the pyridine ring facilitates the formation of an $R_4^3(29)$ ring pattern (Etter, 1990; Etter *et al.*, 1990; Bernstein *et al.*, 1995). These rings are fused to form

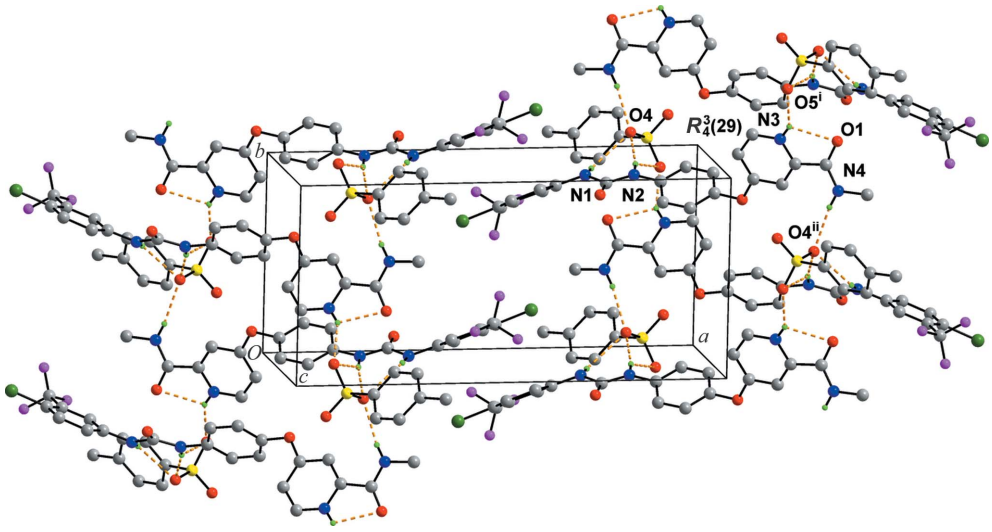

Figure 5
Part of the crystal packing of (II), showing the hydrogen-bonded $R_4^3(29)$ rings fused together to form chains. Hydrogen bonds are shown as dashed lines and H atoms not involved in hydrogen bonding have been omitted for clarity. Selected atoms of the molecules present in the asymmetric unit are labelled, primarily to provide a key for the coding of the atoms. [Symmetry codes: (i) $-x+2, y+\frac{1}{2}, -z+\frac{3}{2}$; (ii) $-x+2, y-\frac{1}{2}, -z+\frac{3}{2}$.]

continuous chains along the *b* axis. The trifluorophenyl rings protrude on the outside of these chains and interdigitate with those from adjacent chains, thereby forming columns populated by halogen atoms.

In conclusion, this structural analysis highlights the variations in the solid-state conformations of the drug and its hydrogen-bonding interactions in different environments.

Experimental

Sorafenib, (I) (Natco Research Centre, Hyderabad) (50 mg), was dissolved in methanol (5 ml). After 2 d, crystals were obtained by slow evaporation. Sorafenib tosylate, (II) (Natco Research Centre, Hyderabad) (50 mg), was dissolved in a mixture of methanol (5 ml) and water (1 ml), and the solution allowed to evaporate slowly. Crystals were obtained after 3 d.

Compound (I)

Crystal data

$C_{21}H_{16}ClF_3N_4O_3$
M_r = 464.83
Monoclinic, $P2_1/c$
a = 8.1587 (16) Å
b = 9.8055 (19) Å
c = 27.758 (5) Å
β = 94.358 (3)°
V = 2214.2 (7) Å^3
Z = 4
Mo $K\alpha$ radiation
μ = 0.23 mm^{-1}
T = 294 K
0.17 × 0.11 × 0.06 mm

Data collection

Bruker SMART APEX CCD area-detector diffractometer
20023 measured reflections
3896 independent reflections
3241 reflections with $I > 2\sigma(I)$
R_{int} = 0.024

Refinement

$R[F^2 > 2\sigma(F^2)]$ = 0.037
$wR(F^2)$ = 0.102
S = 1.02
3896 reflections
302 parameters
H atoms treated by a mixture of independent and constrained refinement
$\Delta\rho_{max}$ = 0.23 e Å^{-3}
$\Delta\rho_{min}$ = −0.17 e Å^{-3}

Table 1
Selected bond distances (Å) and angles (°) for (I) and (II).

	(I)	(II)
C14—C15	1.407 (2)	1.390 (3)
C14—C18	1.419 (2)	1.397 (3)
C15—C16	1.417 (3)	1.367 (3)
C16—N3	1.364 (2)	1.335 (3)
N3—C17	1.368 (2)	1.355 (3)
C17—C18	1.412 (2)	1.369 (3)
C17—C19	1.541 (2)	1.513 (4)
C19—O1	1.263 (2)	1.225 (3)
C19—N4	1.352 (2)	1.320 (4)
C15—C16—N3	124.90 (16)	121.0 (2)
C18—C17—C19	119.66 (14)	128.1 (2)
C18—C17—N3	123.86 (14)	118.9 (2)
C19—C17—N3	116.47 (13)	113.0 (2)
C17—C19—O1	121.34 (14)	118.0 (2)
N4—C19—O1	123.14 (15)	125.4 (3)
C16—N3—C17	116.01 (14)	122.4 (2)
C19—N4—C20	123.45 (16)	121.6 (3)
N4—C19—C17	115.52 (14)	116.6 (2)

Compound (II)

Crystal data

$C_{21}H_{17}ClF_3N_4O_3^+\cdot C_7H_7O_3S^-$
M_r = 637.02
Monoclinic, $P2_1/c$
a = 21.276 (4) Å
b = 9.1160 (17) Å
c = 16.077 (3) Å
β = 108.143 (3)°
V = 2963.2 (10) Å^3
Z = 4
Mo $K\alpha$ radiation
μ = 0.27 mm^{-1}
T = 294 K
0.14 × 0.11 × 0.07 mm

Data collection

Bruker SMART APEX CCD area-detector diffractometer
25287 measured reflections
5198 independent reflections
3604 reflections with $I > 2\sigma(I)$
R_{int} = 0.045

Table 2
Solid-state conformation of sorafenib molecules, indicated by selected torsion angles (°).

Torsion angle	(I)	(II)	3GCS†	3HEG‡	1UWH§ (molecule 1)	1UWH§ (molecule 2)
N4—C19—C17—N3	17.9 (2)	157.7 (2)	7.4	−17.3	24.6	23.0
O1—C19—C17—C18	18.5 (2)	157.0 (3)	7.2	−17.3	−8.6	−9.2
C18—C14—O2—C11	170.80 (15)	−173.0 (2)	−146.3	128.0	151.0	151.7
C14—O2—C11—C12	108.49 (19)	−107.6 (3)	49.7	−42.3	−77.2	−70.3
C12—C13—C8—N2	174.90 (17)	178.1 (2)	−179.6	179.9	−177.7	−176.8
C13—C8—N2—C7	32.6 (3)	13.3 (4)	−148.6	−154.9	−163.9	−151.7
C8—N2—C7—N1	−173.28 (16)	−175.3 (3)	179.5	−162.2	177.2	177.9
N2—C7—N1—C4	−170.62 (17)	167.3 (3)	179.7	−167.9	174.8	174.4
C7—N1—C4—C5	−7.4 (3)	37.7 (5)	−147.3	−157.0	−126.4	−130.1
N1—C4—C5—C6	177.16 (18)	−178.3 (3)	−179.5	−179.7	179.0	179.1

† Simard *et al.* (2009). ‡ Namboodiri *et al.* (2010). § Wan *et al.* (2004).

Table 3
Hydrogen-bond geometry (Å, °) for (I).

D—H···*A*	*D*—H	H···*A*	*D*···*A*	*D*—H···*A*
N1—H1N···O1^{i}	0.86 (2)	2.19 (2)	3.014 (2)	159.0 (18)
N2—H2N···O1^{i}	0.86 (2)	2.15 (2)	2.969 (2)	159.8 (17)
N4—H3N···N3	0.88 (2)	2.34 (2)	2.760 (2)	109.4 (18)

Symmetry code: (i) $-x+1, y-\frac{1}{2}, -z+\frac{3}{2}$.

Table 4
Hydrogen-bond geometry (Å, °) for (II).

D—H···*A*	*D*—H	H···*A*	*D*···*A*	*D*—H···*A*
N1—H1N···O4	0.84 (2)	2.56 (2)	3.234 (3)	138 (2)
N2—H2N···O4	0.83 (2)	2.07 (2)	2.886 (3)	167 (3)
N3—H3N···O1	0.83 (3)	2.28 (3)	2.660 (3)	109 (2)
N3—H3N···O5^{i}	0.83 (3)	2.03 (3)	2.760 (3)	147 (3)
N4—H4N···O4^{ii}	0.85 (2)	2.19 (2)	3.021 (3)	170 (3)

Symmetry codes: (i) $-x+2, y+\frac{1}{2}, -z+\frac{3}{2}$; (ii) $-x+2, y-\frac{1}{2}, -z+\frac{3}{2}$.

Refinement

$R[F^2 > 2\sigma(F^2)] = 0.050$
$wR(F^2) = 0.142$
$S = 1.05$
5198 reflections
406 parameters
3 restraints
H atoms treated by a mixture of independent and constrained refinement
$\Delta\rho_{max} = 0.67$ e Å^{-3}
$\Delta\rho_{min} = -0.53$ e Å^{-3}

All N-bound H atoms were located in a difference Fourier map and their positions and isotropic displacement parameters were refined. All other H atoms were located in a difference density map, but were positioned geometrically and included as riding atoms, with C—H = 0.93–0.96 Å, and with U_{iso}(H) = 1.5U_{eq}(C) for the methyl groups or 1.2U_{eq}(C) for the other H atoms. Distance restraints were applied to N1—H1N, N2—H2N and N4—H4N of (II), with a set value of 0.87 (2) Å. The methyl groups were allowed to rotate but not to tip.

For both compounds, data collection: *SMART* (Bruker, 2001); cell refinement: *SAINT* (Bruker, 2001); data reduction: *SAINT*; program(s) used to solve structure: *SHELXS97* (Sheldrick, 2008); program(s) used to refine structure: *SHELXL97* (Sheldrick, 2008); molecular graphics: *DIAMOND* (Brandenburg & Putz, 2005) and *Mercury* (Macrae *et al.*, 2008); software used to prepare material for publication: *SHELXL97*.

The authors thank Dr J. S. Yadav, Director, IICT, Hyderabad, for his kind encouragement.

Supplementary data for this paper are available from the IUCr electronic archives (Reference: DN3155). Services for accessing these data are described at the back of the journal.

References

Berman, H. M., Westbrook, J., Feng, Z., Gilliland, G., Bhat, T. N., Weissig, H., Shindyalow, I. N. & Bourne, P. E. (2000). *Nucleic Acids Res.* **28**, 235–242.
Bernstein, J., Davis, R. E., Shimoni, L. & Chang, N.-L. (1995). *Angew. Chem. Int. Ed. Engl.* **34**, 1555–1573.
Brandenburg, K. & Putz, H. (2005). *DIAMOND*. Release 3.0c. Crystal Impact GbR, Bonn, Germany.
Bruker (2001). *SAINT* (Version 6.28a) and *SMART* (Version 5.625). Bruker AXS Inc., Madison, Wisconsin, USA.
Escudier, B. *et al.* (2007). *New Engl. J. Med.* **356**, 125–134.
Etter, M. C. (1990). *Acc. Chem. Res.* **23**, 120–126.
Etter, M. C., MacDonald, J. C. & Bernstein, J. (1990). *Acta Cryst.* B**46**, 256–262.
Ferrara, N., Hillan, K. J., Gerber, H. P. & Novotny, W. (2004). *Nat. Rev. Drug Discov.* **3**, 391–400.
Ferrara, N. & Kerbal, R. S. (2005). *Nature (London)*, **438**, 967–974.
Holmes, R., Roberts, O. L., Thomas, A. M. & Cross, M. J. (2007). *Cell. Signal.* **19**, 2003–2012.
Kane, R. C., Farrell, A. T., Madabushi, R., Booth, B., Chattopadhyay, S., Sridhara, R., Justice, R. & Pazudur, R. (2009). *Oncologist*, **14**, 95–100.
Macrae, C. F., Bruno, I. J., Chisholm, J. A., Edgington, P. R., McCabe, P., Pidcock, E., Rodriguez-Monge, L., Taylor, R., van de Streek, J. & Wood, P. A. (2008). *J. Appl. Cryst.* **41**, 466–470.
Namboodiri, H. V., Bukhtiyarova, M., Ramcharan, J., Karpusas, M., Lee, Y. & Springman, E. B. (2010). *Biochemistry*, **49**, 3611–3618.
Ravikumar, K. & Sridhar, B. (2009). *Acta Cryst.* C**65**, o502–o505.
Ravikumar, K. & Sridhar, B. (2010). *Acta Cryst.* C**66**, m35–m39.
Ravikumar, K., Sridhar, B., Krishnan, H. & Singh, A. N. (2008). *Acta Cryst.* C**64**, o15–o17.
Sheldrick, G. M. (2008). *Acta Cryst.* A**64**, 112–122.
Simard, J. R., Getlik, M., Grutter, C., Pawar, V., Wulfert, S., Rabiller, M. & Rauh, D. (2009). *J. Am. Chem. Soc.* **131**, 13286–13296.
Wan, P. T. C., Garnett, M. J., Roe, S. M., Lee, S., Niculescu-Duvaz, D., Good, V. M., Jones, C. M., Marshall, C. J., Springer, C. J., Barford, D. & Marais, R. (2004). *Cell*, **116**, 855–867.
Wilhelm, S. M. *et al.* (2004). *Cell Res.* **64**, 7099–7109.
Yancopoulos, G. D., Davis, S., Gale, N. W., Rudge, J. S., Wiegand, S. J. & Holash, J. (2000). *Nature (London)*, **407**, 242–248.